Proceedings of the SPIE Optical Diagnostics. Wednesday 3 August 2005,
San Diego, CA, USA. Volume 5880, 588011. Eds. Leonard M. Hanssen, Patrick V. Farrell

Single camera three component planar velocity measurements, using two frequency Planar Doppler Velocimetry (2ν-PDV)

Tom O.H. Charrett, Helen D. Ford, Ralph P. Tatam*
Optical Sensors Group, Centre for Photonics and Optical Engineering, School of Engineering,
Cranfield University, Cranfield, Bedford. MK43 0AL, UK

ABSTRACT

The work presented here describes a method that allows three component velocity measurements to be made, quickly and non-intrusively, across a plane in a flow defined by a laser light sheet. The method, two frequency planar Doppler Velocimetry (2ν-PDV) is a modification of the Planar Doppler Velocimetry (PDV) technique, using only a single CCD camera, and sequential illumination of the flow using two frequencies, separated by about 700MHz.
One illumination frequency lies on an absorption line of gaseous iodine, and the other just off the absorption line. The beams sequentially illuminate a plane within a seeded flow and Doppler-shifted scattered light passes through an iodine vapour cell onto the camera. The beam at a frequency off the absorption line is not affected by passage through the cell, and provides a reference image. The other beam encodes the velocity information as a variation in transmission dependent upon the Doppler shift.
Use of a single camera ensures registration of the reference and signal images, which is the major problem in any spilt image system such as a two-camera imaging head, and cost efficiency is improved by the simplification of the system.
A 2ν-PDV system was constructed using a continuous-wave Argon ion laser and acousto-optic modulators to produce two frequencies of illuminating laser light. This was combined with multiple imaging fibre bundles, to port three different views of the measurement plane to a CCD camera, allowing the measurement of three velocity components.

Keywords: Planar Doppler Velocimetry, flow measurement, acousto-optic frequency switching

1. INTRODUCTION

Planar Doppler Velocimetry (PDV)[1-4], also know as Doppler Global Velocimetry (DGV), is a flow measurement technique that provides velocity information over a plane defined by a laser light sheet. PDV relies upon measuring the Doppler frequency shift of light scattered from particles entrained in the flow, and therefore a single observation direction can measure a single component of velocity, as shown in figure 1. However the use of imaging fibre bundles [5] allows several observation directions, and thus velocity components, to be measured simultaneously by spatially multiplexing on to a single CCD camera. The optical frequency shift, $\Delta\nu$, is given by the Doppler equation:

$$\Delta\nu = \frac{\nu(\hat{o} - \hat{i}) \cdot V}{c} \tag{1}$$

where ν is the optical frequency, $\hat{o}$ and $\hat{i}$ are unit vectors in the observation and illumination directions respectively, V is the velocity vector and c is the free space speed of light. The optical frequency of light scattered from each particle in the seeded flow experiences a Doppler shift, which is linearly related to the velocity of the particle. In PDV, a region of the illuminated flow is imaged, through a glass cell usually containing iodine vapour, onto the active area of a CCD camera. Iodine has numerous narrow absorption lines over a large part of the visible spectrum[6] and the laser frequency is chosen to coincide with one such line. Hence the optical intensity at any position in the camera image is a function of the Doppler shift experienced at the corresponding position in the flow, via the frequency-dependent iodine absorption.

* r.p.tatam@cranfield.ac.uk; phone +44 (0) 1234 754630; fax +44 (0) 1234 752452;
http://www.cranfield.ac.uk/soe/cpoe

Optical Diagnostics, edited by Leonard M. Hanssen, Patrick V. Farrell, Proceedings of SPIE Vol. 5880
(SPIE, Bellingham, WA, 2005) · 0277-786X/05/$15 · doi: 10.1117/12.614380

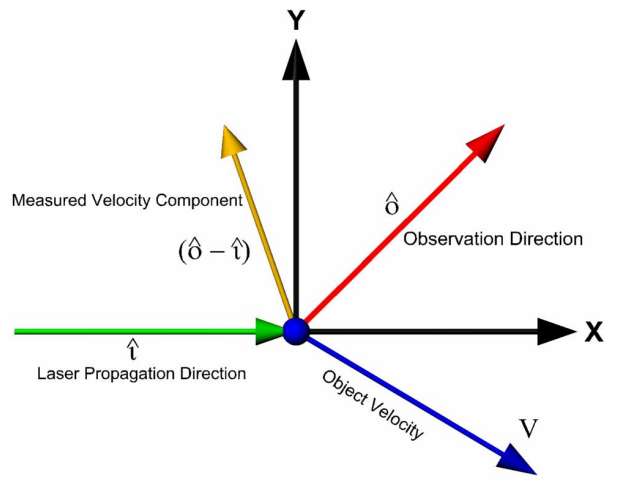

Figure 1. The relationship of laser illumination direction and observation direction to the measured velocity component determined from the Doppler equation. Where $\hat{\boldsymbol{o}}$ and $\hat{\boldsymbol{i}}$ are unit vectors in the observation and illumination directions respectively.

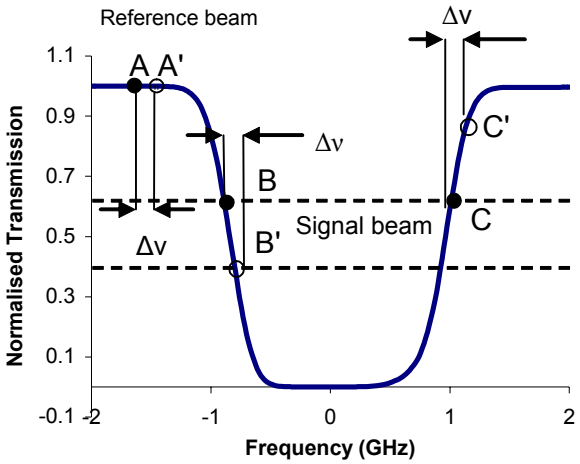

Figure 2. Relative positions of the laser frequency, and the shifted frequency on a typical absorption feature for 2ν-PDV (A and B/C denote the position of the illumination frequencies and A' and B'/C' the Doppler shifted frequency.)

The intensity over a PDV image is also affected by the intensity profile of the illuminating laser sheet (typically Gaussian), spatial variations of the seeding density within the flow, and diffraction fringes caused by imperfections in the optical surfaces. These variations are generally of similar amplitude to those resulting from absorption in the iodine cell, and can obscure the information about flow velocity that is contained within the camera image. It is therefore usual to amplitude-divide the image beam onto two cameras; from one of the two imaging paths the iodine cell is omitted, and the resulting image acts as a reference to normalize the signal image carrying the velocity information.

Viewing the flow from a single observation direction allows a single component of the flow velocity to be measured; therefore to make three-dimensional measurements a minimum of three viewing directions are necessary. Conventional methods use a separate PDV imaging head (two cameras and an iodine cell each) to measure each of the three velocity components. The use of imaging fibre bundles, to port multiple views of the region of interest to a single detector head, considerably simplifies the system and makes it possible to make three component velocity measurements using a single PDV imaging head.

2. TWO FREQUENCY PLANAR DOPPLER VELOCIMETRY (2ν-PDV)

In the two-frequency Planar Doppler Velocimetry (2ν-PDV)[7-9] technique the signal and reference images are acquired sequentially, on the same CCD camera by the use of two illumination frequencies. There are two approaches.

In the first approach the first illumination frequency is tuned just off the low frequency side of an absorption line to lie in a zero absorption region of the iodine transfer function (figure 2, point A). A reference image is then acquired. The second illumination frequency is positioned at approximately midway (50%) on the iodine cell transfer function (figure 2, point B), and a signal image is acquired. The two images can then be processed as in conventional PDV.

The two frequencies can be generated from a single laser source using a combination of acousto-optic modulators (AOMs) to shift the laser frequency or by tuning the laser frequency directly. The optical frequency difference is typically ~700MHz, which is sufficiently small that there will be no change in the scattering for the size of particles typically used; 0.2-5 μm diameter.

Exact alignment of the reference and signal images on the active area of the camera is automatic. This avoids the signal/reference image misalignment problem found in conventional PDV where superposition of the two images to sub-

pixel accuracy is essential if errors in the calculated velocities are to be minimized. For example Thorpe et al [10] assess the impact of image misalignment, on the velocity field of a rotating disc, for an image misalignment of 0.1 pixels, they give an estimate of this error as ± 5ms^{-1}. Errors due to poor image registration become particularly troublesome if large velocity gradients are present in the region imaged. The main causes of poor image registration are differences between the optical aberrations and magnifications of the two imaging paths so errors tend to be worse towards the outside edges of the images, where these factors are largest.

The method also eliminates the polarization sensitivity of the split ratio of the beam splitter used in two-camera systems[10]. Ideally the beam splitter used in a conventional PDV imaging head would split the incoming light 50:50 between the signal and reference cameras with no variation for different polarisations of light. However even the 'non-polarising' beam splitters typically used retain a slight sensitivity to polarisation, typically quoted as ±3% variation in the split ratio for S and P polarized light, leading to typical velocity errors of ±7ms^{-1}.

The second approach increases the sensitivity of the system by tuning the two frequencies to the positions shown as B and C in figure 2. With one source tuned onto the falling slope and the other on the rising slope, a constant Doppler shift will result in the further attenuation of one image to a lower signal level and the rise in the signal level in the other image. Dividing the difference of the images by the sum, and taking into account any difference in the gradients will give a result that has approximately double the sensitivity of the current PDV methods.

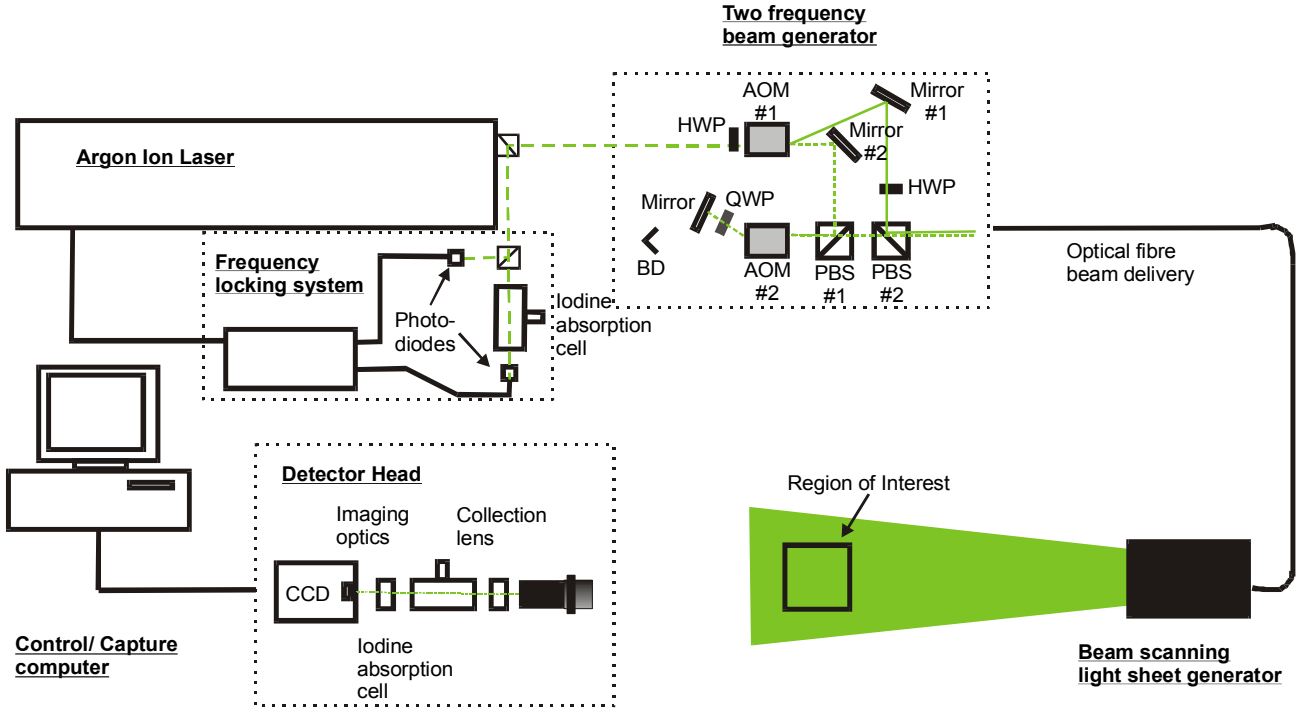

Figure 3. Schematic of the experimental arrangement for the single component measurements including detail of the two-frequency beam generator showing the generation of both the signal and reference beams.

HWP - λ/2 plate; AOM – acousto-optic modulator; PBS – polarising beam splitter, QWP – λ/4 plate; BD – beam dump. ——— Reference beam path ····· Signal beam path – – – Un-shifted laser beam

3. SINGLE VELOCITY COMPONENT MEASUREMENTS

Initially the system was set-up to measure a single velocity component as shown in figure 3. A continuous wave argon ion laser was used as the light source, allowing time averaged velocity measurements to be made. The optical frequency of this source was altered to form the reference and signal beams using a combination of two acousto-optic modulators

(AOM). The generation of both the reference beam and the signal beam is shown in the detail of the two-frequency beam generator. The signal beam is generated when AOM 1 is switched on and AOM 2 is switched off, providing an up-shift of 520MHz. When AOM 2 is on and AOM 1 off the reference beam is generated with a 180MHz downshift in frequency.

Both beams leave the beam generator and are coupled into an optical fibre. The beams are then delivered to a prism-scanning device[11]. This scans the collimated beam rapidly across the region of interest, resulting in an ideal 'top-hat' intensity profile of the generated light sheet. The desired illumination frequency can then be selected by toggling on/off the two AOMs.

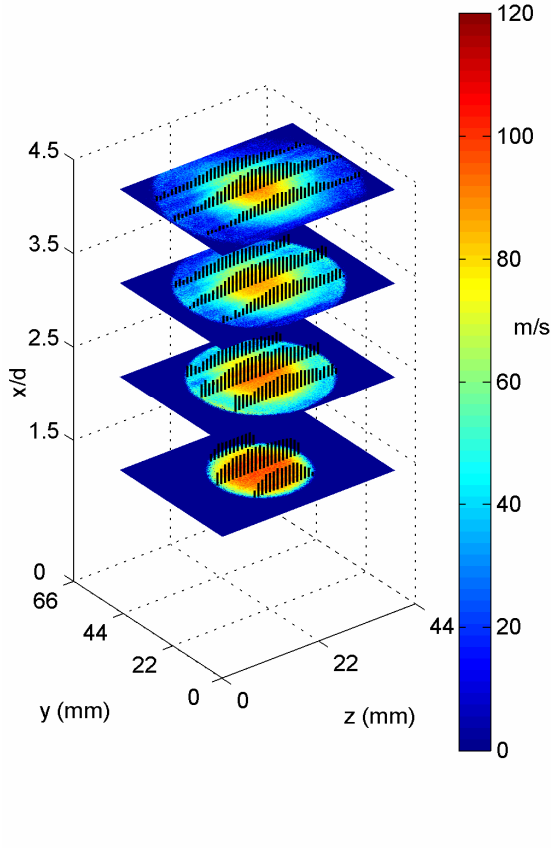

Figure 4. The velocity field of an axisymmetric air jet made using 2ν-PDV. Measurements were taken at 1.5, 2.5, 3.5 and 4.5 nozzle diameters downstream from the nozzle. Overlaid are vectors showing the magnitude of the velocity at various points (arrow heads have been removed for clarity)

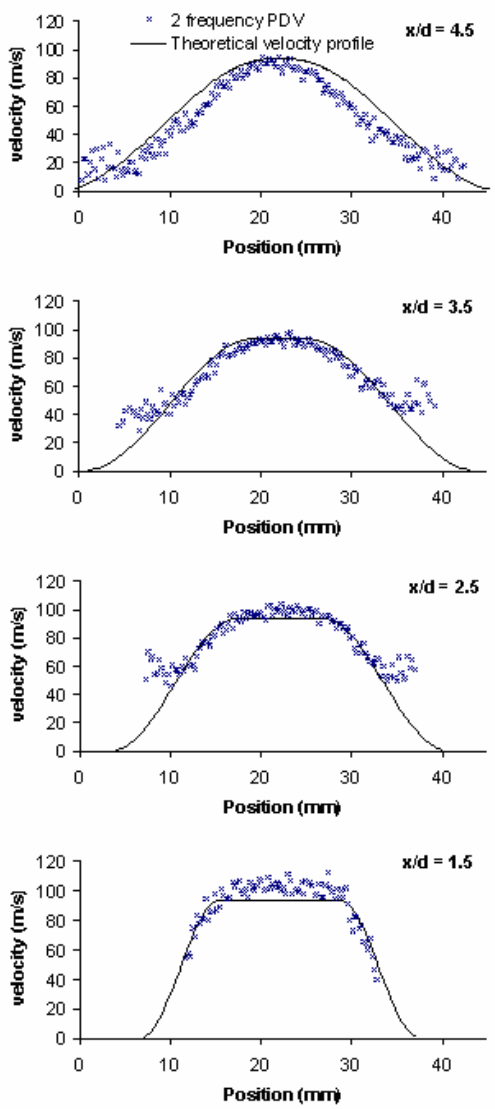

Figure 5. Profiles taken through the centre of each slice shown in figure 4, (crosses – experimental values, solid – theoretical velocity profile). x/d = nozzle diameters downstream.

A frequency locking system is used to control the laser's fundamental frequency, and hence the positions of the two beams on the iodine absorption line. This consists of an iodine cell, signal and reference photodiodes and locking electronics which adjusts the laser etalon temperature to ensure that the laser frequency is stable, based upon the transmission through this cell.

The detector head images the region of interest in the flow using a standard SLR camera lens and a signal image and a reference image are captured under the appropriate illumination selected by toggled the AOMs on/off. It was then demonstrated on an axis-symmetric air jet, with a 20mm diameter smooth contraction nozzle that was seeded using a smoke generator producing particles in the 0.2-0.3μm diameter range. The jet has a theoretical exit velocity of $94ms^{-1}$, which was calculated by measuring the nozzle pressure ratio. Figure 4 shows the main velocity component of this jet at various positions from the nozzle[7] and figure 5 shows profiles taken through the centre of each slice compared with the theoretical velocity profile for the jet. It can be seen that the results agree well with the calculated profiles. The larger variation between the profiles at the edges of the jet is a result of less seed particles being present in this region. This resulted in less scattered light and lower signal levels.

4. THREE COMPONENT VELOCITY MEASURMENTS

The system was then extended to measure three velocity components, using the imaging fibre bundles as the input into the detector head. Views of the region of interest are ported to the detector head using a coherent array of fibres that is split into four channels (figure 6). Each channel has 600x500 fibres that are 8μm in diameter and positioned at 10μm centres. These views are combined at the detector head, with each occupying a quarter of the CCD image (figure 7). An example of the image formed is shown in figure 8. This is a view of a calibration target used to de-warp the image to a common view and determine the observation directions for each view[5]. Figure 9 shows the result after this de-warping process; here all four views have been overlaid for demonstration purposes.

Figure 6. The individual arms of the imaging fibre bundles.

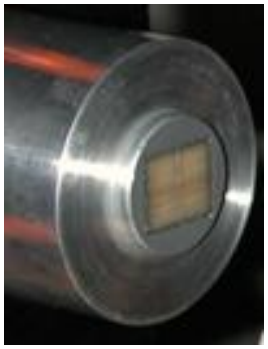

Figure 7. The combined end of the imaging fibre bundles.

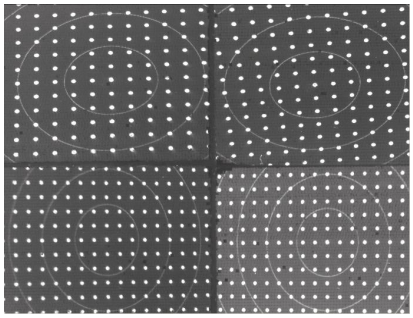

Figure 8. An example image of a view through the imaging bundles of a calibration target (field of view ~100 x 100 mm)

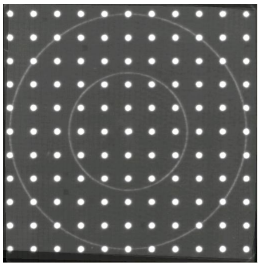

Figure 9. An example of the 'de-warped' views, showing all four views overlaid

The arrangement of the beam generator, shown in figure 3, was very light inefficient and combined with the use of the imaging fibre bundles, resulted in low scattered light levels being collected. The experimental arrangement was modified to allow greater illumination power; this new arrangement is shown in figure 10. Here the laser frequency is selected by tuning the laser etalon voltage and is then stabilized using the locking system described above. The frequency of the locking beam is shifted by 260MHz, using an acousto-optic modulator, so that the locking system can still operate if the

laser is located at 100% transmission. The locking beam will be shifted onto the absorption line so that any frequency fluctuations will result in a transmission fluctuation seen by the photodiodes and can be corrected for. Although this arrangement increased the illumination power the images are now captured with a separation of minutes rather than seconds, although for time average measurements this has not proved to be a problem.

As well as providing increased beam powers, it is now possible to tune both beam frequencies to coincide with either side of the absorption line. This was not possible using the two-frequency beam generator described in section 3, as a frequency separation of greater than 700MHz is required to span the absorption line. The ability to do this allowed increased sensitivity measurements to be made as described in section 2.

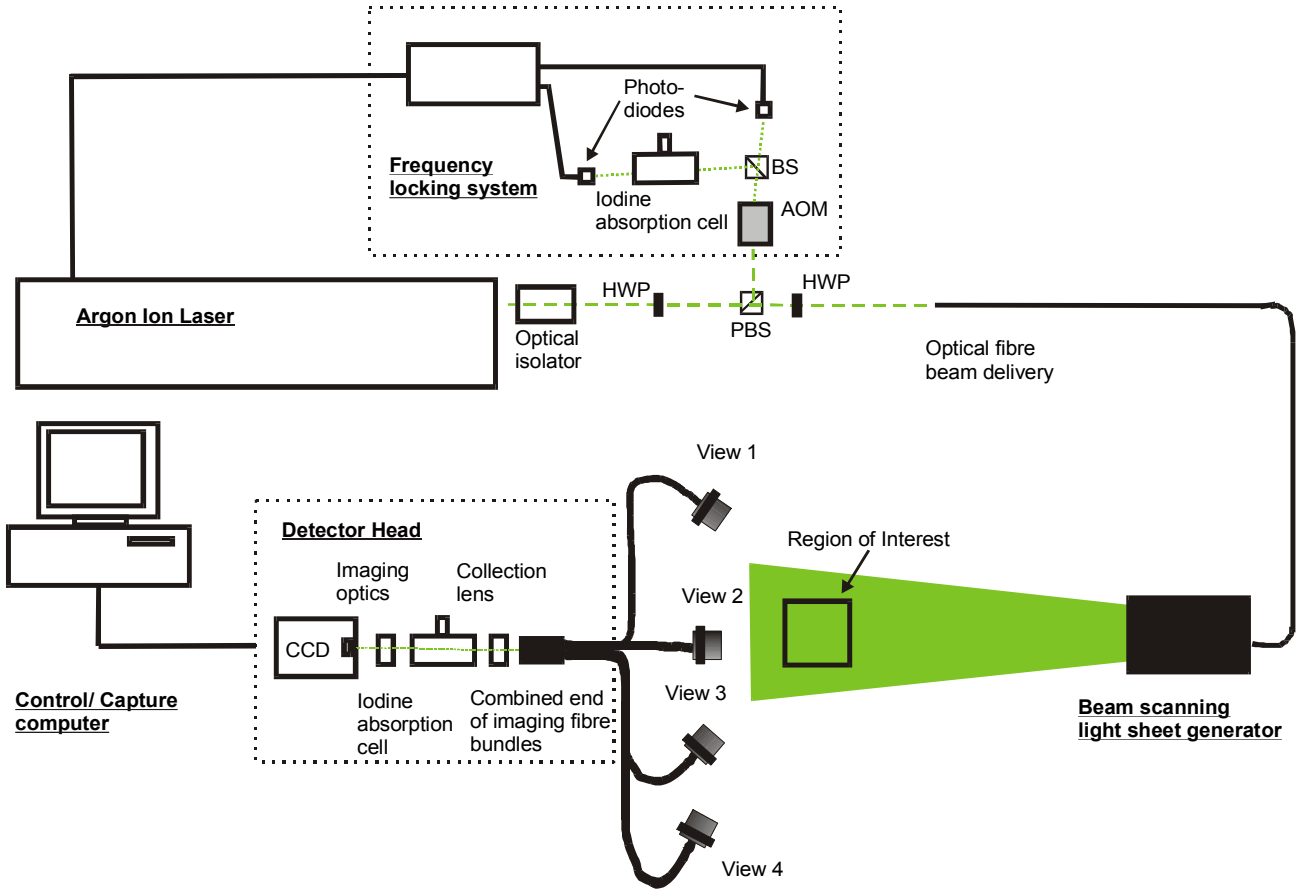

Figure 10. Schematic showing the experimental arrangement used for the three dimensional velocity measurements.

HWP - λ/2 plate; AOM – acousto-optic modulator; PBS – polarising beam splitter, ····· Shifted (locking) beam path – – – Un-shifted (illumination) beam

A further modification to the system was that the multi-mode fibre used in the single component measurements to transport the beams to the light sheet generator, was replaced with a single-mode, polarization-preserving fibre. This was changed to ensure that the spatial profile of both beams remained the same. If these differ significantly, the illumination profiles can also differ, especially when a thick sheet is required, such as when illuminating the face of disc; previously when making single component measurements on the disc it was noted that a 'white card' correction was needed[7].

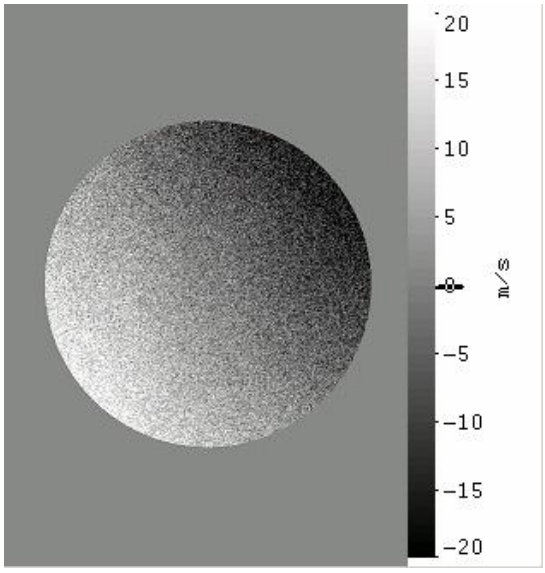

Figure 11 – A single measured velocity component of a rotating disc, calculated using the normal sensitivity scheme.

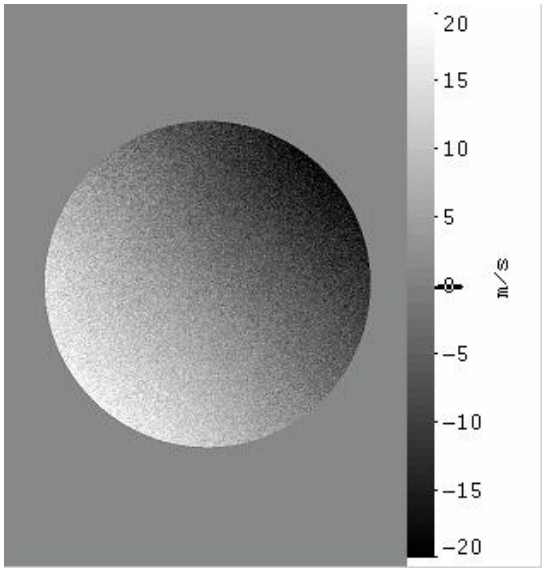

Figure 12 – A single measured velocity component of a rotating disc, calculated using the increased sensitivity scheme.

The system was used to measure the velocity field of a rotating disc. This provides a well-known velocity field with which to characterise the performance of the system. Each arm of the imaging fibre bundle was used with a standard SLR camera lens to view the rotating disc. The disc itself was 200mm in diameter, although the common field of view of each observation direction was an approximate disc 100mm in diameter. The rotation of the disc was measured using an optical tachometer giving a maximum velocity in the field of view of ~34ms^{-1}.

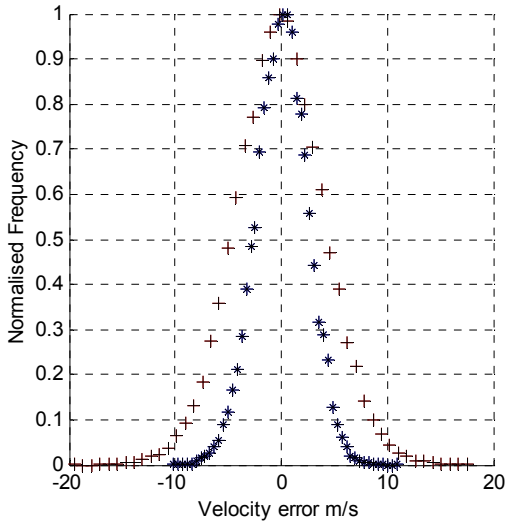

Figure 13 – Histograms of the variation between the measured velocity component and the theoretical velocity component for a rotating disc
+ Normal sensitivity 2ν-PDV technique.
* Increased sensitivity 2ν-PDV technique.

Measurements were made using both the reference/signal (normal sensitivity) and signal/signal (increased sensitivity) two frequency PDV methods. Each observation direction was processed to yield the measured velocity component given by ***(ô – î)***. Figures 11 and 12 show a single measured velocity component for the normal and increased sensitivity schemes.

The adoption of a single mode fibre for transporting the beam from the two-frequency beam generator to the sheet forming optics, results in identical signal and reference illumination profiles and there being no need to apply the 'white card' correction to realise the velocity field. This also meant that the low-pass filtering commonly used in PDV processing could be kept to a minimum, with no filtering at all applied to these results.

It can be seen that the velocity component captured using the increased sensitivity scheme is considerable smoother than that captured using the normal reference/signal scheme.

The benefit of this scheme can also be seen when subtracting the theoretical velocity component from the experimental velocity component. Figure 13 shows a histogram (normalised frequency vs. velocity error) of this subtraction, with the increased sensitivity scheme having significantly less variation. This is also the case for the other three components that were measured using the other channels of the imaging fibre bundle. The standard deviations of this variation are shown in Table 1 for both the normal and increased sensitivity schemes. It can be seen that there is approximately a 40% reduction in the error when using the increased sensitivity scheme over the normal sensitivity scheme.

Table 1 – Standard deviations of the variation between the measured and theoretical velocity components, and the calculated reduction in error when using the increased sensitivity scheme.

Standard deviation	View 1	View 2	View 3	View 4
Normal sensitivity	4.88 ms^{-1}	5.30 ms^{-1}	2.56 ms^{-1}	4.16 ms^{-1}
Increased sensitivity	2.73 ms^{-1}	3.10 ms^{-1}	1.63 ms^{-1}	2.46 ms^{-1}
% Reduction	44%	41.5%	36.3%	40.9%

The measured velocity components are then converted to the orthogonal velocity components U, V and W, representing the vertical, horizontal and out-of-plane components. Figure 14 shows a comparison between the two sensitivity schemes for these orthogonal velocity components. The improved sensitivity can also be seen in these calculated orthogonal components with the increased sensitivity results being visibly smoother. Again if the calculated components are compared with the theoretical components and histograms taken of this variation, the increased sensitivity scheme makes a considerable improvement. The standard deviations of this, shown in table 2, are again typically 40% smaller for the increased sensitivity scheme compared with the normal sensitivity scheme, as would be expected from the improvement in the measured velocity components

Table 2 – Standard deviations of the variation between the calculated and theoretical orthogonal velocity components, and the calculated reduction in error when using the increased sensitivity scheme.

Standard deviation	U	V	W
Normal sensitivity	4.08 ms^{-1}	7.07 ms^{-1}	6.29 ms^{-1}
Increased sensitivity	2.31 ms^{-1}	4.19 ms^{-1}	3.34 ms^{-1}
% Reduction	43.3%	40.6%	46.8%

It should be noted that the process of converting the measured velocity components to the three orthogonal components will magnify the error present. This results in the errors in the orthogonal components being greater than those in a single velocity component measurement. The viewing configuration used for disc measurements is far from ideal due to the restriction of only being able to view the light sheet (the face of the disc) from a single side, so this magnification is greater than it would be for real seeded flow experiments where the light sheet can be viewed from both sides.

5. CONCLUSIONS

A PDV technique using two illumination frequencies and imaging fibre bundles has been demonstrated that is capable of measuring all three components of velocity, across a plane defined by a light sheet, using a single CCD camera. Single velocity component, time averaged, velocity measurements on a rotating disc and a seeded air jet were made and the pixel-matching problem has been overcome by the use of a single camera. This results in there being no need to use a 'white card' correction commonly applied in PDV measurements.

The potential to expand the system to measure all three components of velocity, using imaging fibre bundles, has been demonstrated by making measurements of a rotating disc. The use of the imaging fibre bundles also allows greater flexibility in the positioning of the observation directions.

The ability to further improve the sensitivity of the two-frequency PDV technique, by positioning both illumination frequencies on opposite sides of the transfer function, has been demonstrated. By comparison with the theoretical velocity field for a rotating disc a typical reduction in the error of approximately 40% can be achieved.

ACKNOWLEDGEMENTS

This work was funded by the Engineering and Physical Sciences Research Council (EPSRC), UK (GR/SO4291).

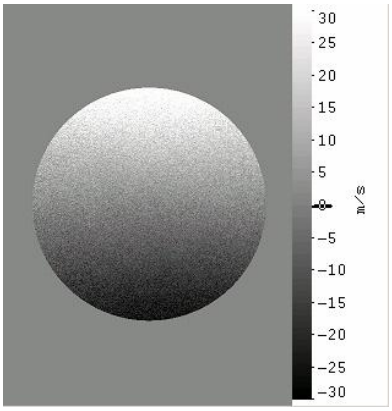

U (normal sensitivity)

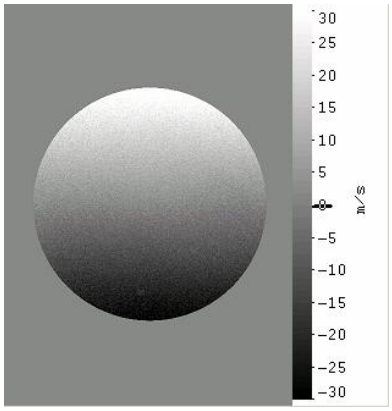

U (increased sensitivity)

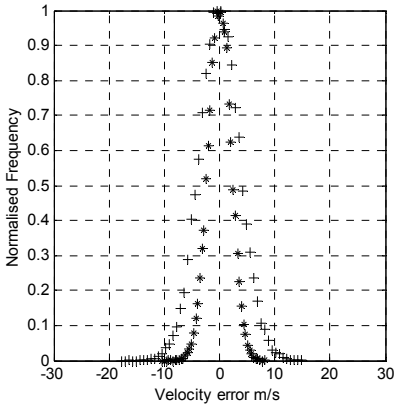

U error

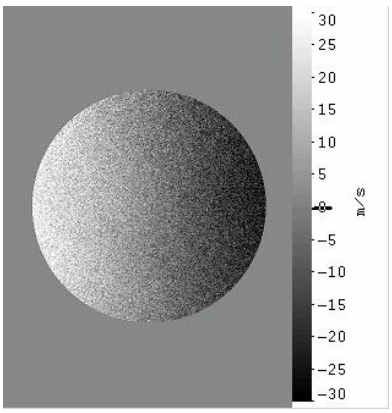

V (normal sensitivity)

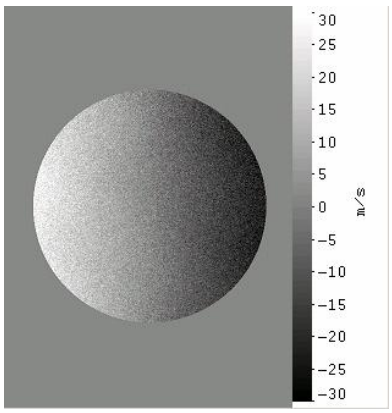

V (increased sensitivity)

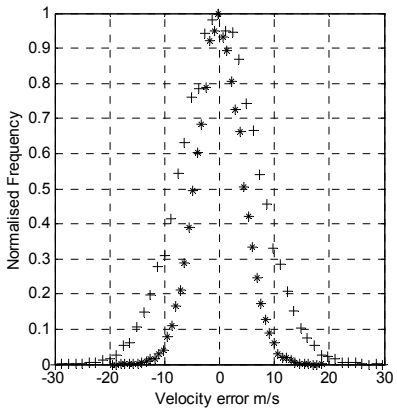

V error

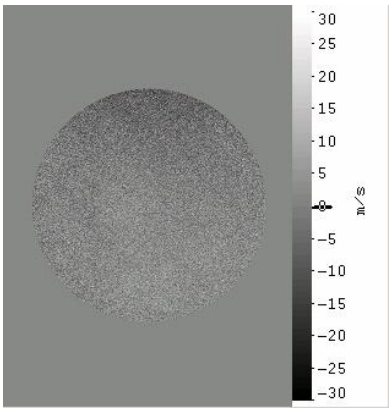

W (normal sensitivity)

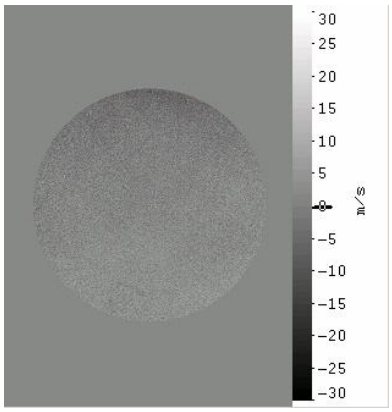

W (increased sensitivity)

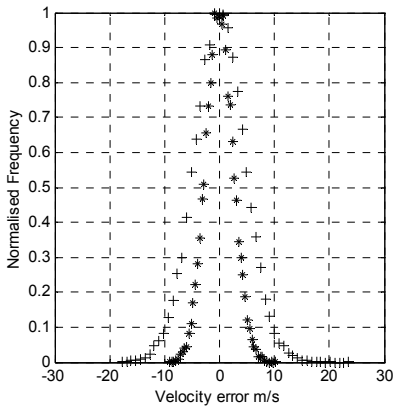

W error

Figure 14 – Comparison of computed orthogonal velocity components; (left column) Examples of the calculated orthogonal velocity components using the normal sensitivity 2ν-PDV technique; (middle column) Examples of the calculated orthogonal velocity components using the increased sensitivity 2ν-PDV technique; (right column) Histograms showing the difference between the measured and theoretical velocity component. + Normal sensitivity 2ν-PDV technique. * Increased sensitivity 2ν-PDV technique.

REFERENCES

1. Komine, H., Brosnan, S., Litton, A., and Staepperts, E., "Real-Time Doppler Global Velocimetry", *AIAA 29th Aerospace Sciences Meeting,* Reno, Nevada , Paper 91-0337, 1991.

2. Meyers, J.F. and Lee, J.W., "Proof of concept test of the Doppler Global Velocimeter", *Spaceborne Photonics: Aerospace Applications Of Lasers And Electro-optics*, Newport Beach, CA, 1991.

3. Meyers, J.F., Lee, J.W., and Schwartz, R.J., "Characterization of Measurement Error Sources in Doppler Global Velocimetry", *Measurement Science and Technology,* **12**, 357-368, 2001.

4. Ford, H.D. and Tatam, R.P., "Development of Extended Field Doppler Velocimetry for Turbomachinery Applications", *Optics and Lasers in Engineering,* **27** , 675-696, 1997.

5. Nobes, D.S., Ford, H.D., and Tatam, R.P., "Three Component Planar Doppler Velocimetry Using Imaging Fibre Bundles", *Experiments in Fluids,* **36**, 1, 3-10, 2004.

6. Gerstenkorn, S. and Luc, P., *Atlas du Spectre d'Absorption de la Molecule d'Iode 14800-200 cm^{-1} Complement: Identification des Transitions du Systeme (B-X)*,Editions du Centre Nationale de la Recherche Scientifique, Paris, France, 1986

7. Charrett, T.O.H., Ford, H.D., Nobes, D.S., and Tatam, R.P., "Two frequency Planar Doppler Velocimetry (2υ-PDV)", *Review of Scientific Instruments,* **75**, 11, 4487-4496, 2004.

8. Charrett, T.O.H., Ford, H.D., Nobes, D.S., and Tatam, R.P., "Dual Illumination Planar Doppler Velocimetry using a Single Camera", *Optical Diagnostics for Fluids, Solids, and Combustions II, Proceedings of the Society of Photo-optical Instrumentation Engineers (SPIE)*, San Diego, CA, paper 5191, pp 113-121, 2003.

9. Charrett, T.O.H., Ford, H.D., Nobes, D.S., and Tatam, R.P., "Two-Frequency Planar Doppler Velocimetry (2v-PDV)", *12th International symposium on the application of Laser Techniques to fluids*, Lisbon, 2004.

10. Thorpe, S.J. , Ainsworth, R.W., and Manners, R.J., "The Development of a Doppler Global Velocimeter and its Application to a Free Jet Flow", *ASME / JSME Fluids Engineering and Laser Anemometry Conference and Exhibition*, Hilton Head, SC, USA, 1995.

11. Roehle, I., Willert, C., Schodl, R., and Voigt, P., "Recent Developments and Applications of Quantitative Laser Light Sheet Measuring Techniques in Turbo machinery Components", *Measurement Science and Technology,* **11**, 1023-1035, 2000.